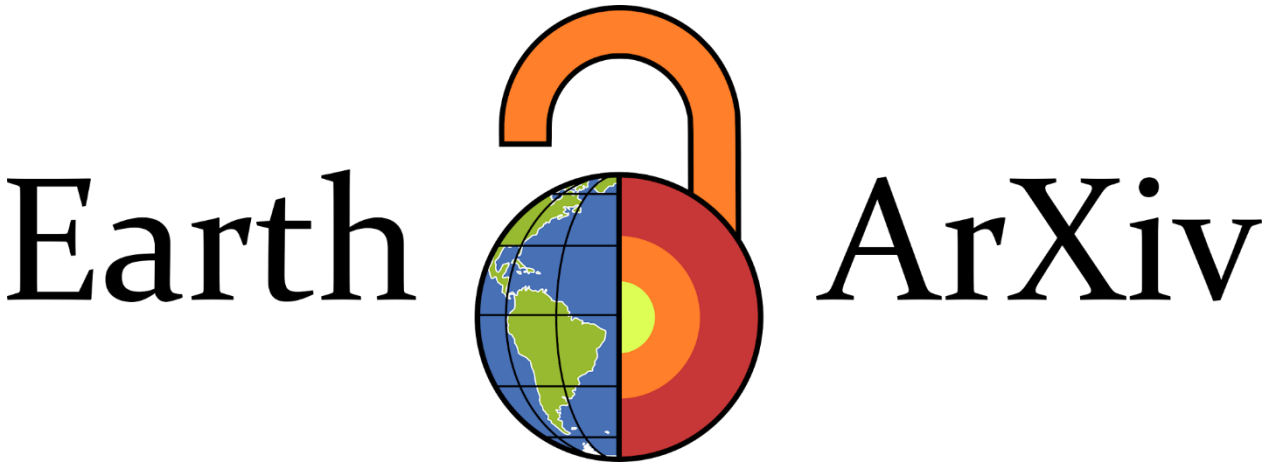

Kaolin as a potential lithium source: a preliminary study of the Torniella ceramic raw material deposit (southern Tuscany)

Sara Longo[1], Pilario Costagliola[2], Pierfranco Lattanzi[3], Marta Morana[2], Guia Morelli[3], Massimiliano Reginelli[4], Valentina Rimondi[2] & Simona Raneri[2]

[1]Consorzio Interuniversitario Nazionale per la Scienza e Tecnologia dei Materiali, via G. Giusti 9, Firenze.
[2]Dipartimento di Scienze della Terra, Università degli Studi di Firenze, via G. La Pira 4, Firenze.
[3]Consiglio Nazionale delle Ricerche - CNR, Istituto di Geoscienze e Georisorse - IGG, via G. La Pira 4, Firenze.
[4]Eurit Srl, Località Buraccio 6, Porto Azzurro (LI).

SL, 0009-0008-4823-7388; PC, 0000-0003-3557-8091; PL, 0000-0003-4352-2709; MM, 0000-0002-5724-9216; GM, 0000-0001-5467-325X; VR, 0000-0002-1249-6563; SR, 0000-0002-3135-7083.

Corresponding author e-mail: simona.raneri@unifi.it

ABSTRACT

The Torniella ceramic raw material deposit (southern Tuscany) is hosted within highly altered rhyolites of the Tertiary Tuscan magmatic province. Locally, kaolinite-rich veins occur, consisting of >80% kaolinite, with minor quartz and traces of svanbergite, $SrAl_3(PO_4)(SO_4)(OH)_6$. The bulk vein material shows interesting lithium (Li) contents, ranging from 1600 to 3700 mg/kg, with local enrichment up to 6000 mg/kg. Preliminary experiments to assess the potential for Li extraction resulted in negligible release (0.2-0.4%) at room temperature (reaction with pure water, 1M $MgCl_2$ solution, and 1M HCl solution). Roasting at 600 °C and leaching with oxalic acid resulted in up to 60% Li recovery. Conversely, roasting at 850 °C with sodium sulfate and water leaching yielded a lower Li recovery (~40%). These results suggest that Li can be effectively mobilised only after thermal activation. While the local resource is limited and the deposit itself is unlikely to be economically viable, this study acknowledges the potential of Li recovery as a by-product of kaolin extraction for the ceramic industry.

KEYWORDS: lithium, kaolin, Torniella, lithium extraction.

INTRODUCTION

Lithium (Li) is included among the European Union list of critical raw materials primarily due to its significance in battery technologies (European Parliament, 2024). At a global scale, the main producers of Li ores are Argentina, Australia, Chile, China, and Zimbabwe (U.S. Geological Survey, 2026). Conventionally, Li extraction has relied on two primary resources: continental brines (*salares*) and granitic pegmatites (Benson et al., 2025). A third type of deposits, referred to as either clay-type deposits (Bowell et al., 2020) or volcano-sedimentary deposits (Putzolu et al., 2025), has recently attracted increasing attention, especially because some prospects, such as Thacker Pass (Nevada), or Jadar (Serbia), contain estimated reserves exceeding 1 Mt Li. Jadar represents a notable exception, where the Li-bearing phase is the unique mineral jadarite. However, in the majority of clay-type deposits, Li is predominantly associated with clay minerals or micas, where it frequently substitutes for Mg^{2+} in octahedral sites, as observed in hectorite ($Na_{0.3}(Mg,Li)_3Si_4O_{10}(OH)$), or tainiolite ($KLiMg_2Si_4O_{10}F$). Finally, lithium has been observed to occur adsorbed on the clay mineral surfaces or as an interlayer cation (e.g., Benson et al., 2023; Yan et al., 2025). In principle, kaolinite is not considered to be a favourable host for lithium (e.g., Starkey, 1982). Substitution in the octahedral sites is limited by the large charge difference between Li^+ and Al^{3+}, while the theoretical absence of interlayer cations and the relatively low cation exchange capacity should restrict Li incorporation through adsorption. Indeed, sorption experiments by Hoyer et al. (2015) found that, under identical conditions, kaolinite takes up about one third of lithium with respect to bentonite and zeolite. Nonetheless, natural kaolinite containing hundreds to even thousands of µg/g Li has been reported (Hoyer et al., 2015; Hao et al., 2025), and there has been some recent attention, especially from Chinese researchers, to the potential recovery of Li from kaolinite-bearing rocks (e.g., Zhong et al., 2024).

A joint research group at the Department of Earth Sciences, University of Florence, and at the Institute of Geosciences and Georesources (CNR) was recently involved in two companion projects (ARTÙ and LiCycle) aimed at the recovery of lithium from mine by-products and industrial non-compliant materials generated along the ceramic industry supply chain. Specifically, one of the goals of the ARTÙ project is exploring the potential recovery of lithium and other critical metals from rocks quarried

at the ceramic raw material mines of *La Crocetta* (Porto Azzurro, LI, Elba Island) and *I Piloni* (Torniella, GR, Tuscany), run by the EURIT Srl company (http://euritonline.com/prodotti.html). Run-of-the-mine bulk rocks, including rhyolites with varying degrees of alteration from Torniella mine and aplites (commercially known as eurite) from Elba Island, were characterised from petrographic, mineralogical, and geochemical perspectives. Preliminary studies on these lithotypes evidenced that no specific mineralogical phases associated with lithium could be identified, while optical emission spectrometry (ICP-OES) detected Li contents ranging from 35 to 180 mg/kg in rhyolites from Torniella, and between 119 and 169 mg/kg in aplites from Elba Island (Finto, 2025). These values exceed the mean Li content of the upper continental crust (41 ± 6 mg/kg, Hu & Gao, 2008), and are consistent with the documented Li anomaly within the products of the Tuscan magmatic province (Dini et al., 2022). Notably, elevated Li contents were detected in samples from apparently pure kaolin veins at Torniella, up to 3000 mg/kg (Finto, 2025), i.e. markedly higher than the known Li anomaly within products of the Tuscan magmatic province (Dini et al., 2022). In this study, further laboratory investigations were conducted on pure kaolin veins from Torniella mine to assess lithium concentrations in these secondary assemblages and to explore the application of sustainable Li extraction methods. It should be noted that these results are preliminary; further analyses are required for a comprehensive characterisation.

GEOLOGICAL CONTEXT

The Torniella (*I Piloni*) mine near Roccastrada (GR) is one of the most significant deposits of kaolin in Italy (Lombardi & Mattias, 1987; Viti et al., 2007; Sammuri & Scapigliati, 2022) (Fig. 1). It is developed within rhyolitic rocks of the Tuscan Magmatic Province, which are interpreted as the product of crustal anatexis and represent one of the most evolved and silica-rich magmatic products of the province (Mazzuoli, 1967; Pinarelli et al., 1989). The volcanic rocks crop out south of Torniella as a NW-SE elongated body, roughly 3 km wide, whose western margin is controlled by a tectonic contact associated with a NW-SE fault system; later SW-NE faults intersect the volcanic body, locally influencing the structural framework of the area. The rhyolites are affected by variable degrees of hydrothermal alteration, producing lithologies that range from relatively well-preserved volcanic rocks to strongly kaolinized materials. At present, a systematic description of the spatial distribution of alteration is lacking. Broadly speaking, the phenomenon is associated with fractures mainly controlled by the Apennine and anti-Apennine fault system (Mazzuoli, 1967; Bertolani & Loschi Ghittoni, 1989). The resulting mineral assemblage is relatively uniform, characterised by secondary kaolinite and alunite (and other minerals of the alunite supergroup), along with relict primary minerals such as quartz and sanidine. Alunite has been mined in the past, but nowadays it compromises the quality of the ore. Based on its isotopic composition ($\delta^{34}S$ values ranging from +6.7 to +9.6 per mil), Cortecci et al. (1981) suggested that alunite at Torniella results from supergene oxidation of sulfides. However, there is no evidence that sulfides were ever present at Torniella. An alternative explanation is the oxidation of H_2S upon reaction of ascending H_2S-bearing steam with cool groundwater (steam-heated environment; cf. Rye et al., 1992; Hedenquist & Arribas, 2022). The kaolinite-alunite acid-sulfate alteration assemblage is comparable to that described in the Tolfa district (Lombardi & Mattias, 1979). The uneven distribution of alunite at the Torniella mine reflects local variations in fluid chemistry, particularly in the availability of sulfur components

(Lattanzi et al., 2001). In addition to the primary hydrothermal deposition, minor occurrences of sedimentary kaolinite have been identified within small, post-orogenic lacustrine basins to the south of the mine (Bertolani & Loschi Ghittoni, 1989). These deposits were formed through the erosion and redeposition of kaolin derived from altered rhyolitic rocks. Alunite is scarce or absent in these occurrences, which improves their economic quality (Lombardi & Mattias, 1987; Bertolani & Loschi Ghittoni, 1989).

Currently, Torniella mine is exploited in different sectors, characterised by rhyolites from intact to intensely altered. Specifically, sectors B and D of the mine exhibit considerable lithological variability, ranging from well-preserved rhyolites to strongly kaolinized materials. In sector B, the rhyolitic formation exhibits localised fracture systems containing kaolin veins. The fractures are predominantly sub-vertical, although sub-horizontal fractures with variable orientations are also present. Kaolin veins range in thickness from a few millimetres to 2-3 cm, with isolated others reaching 4-5 cm (Fig. 2). They are currently considered part of the mineable material. The relatively low iron content (see Tab. 3 below) is advantageous for industrial applications, whereas the local occurrence of sulfate minerals is a disadvantage. Petrographic observations indicate that the Torniella rhyolites are characterised by a porphyritic texture with a fractured glassy groundmass hosting abundant phenocrysts of quartz and K-feldspar (up to centimetric), with minor occurrence of plagioclase and biotite flakes (Viti et al., 2007; Finto, 2025). In the less altered samples, the primary mineral assemblage is largely preserved, although plagioclase and K-feldspar locally exhibit early alteration features, including fracturing and partial replacement by secondary phases. In strongly altered rhyolites, plagioclase and biotite are completely replaced, and the groundmass develops a microgranular texture dominated by kaolinite, whereas quartz and K-feldspar phenocrysts remain as relic grains. In the fracture-hosted kaolin veins, the mineral assemblage is dominated by kaolinite, with minor quartz and K-feldspar.

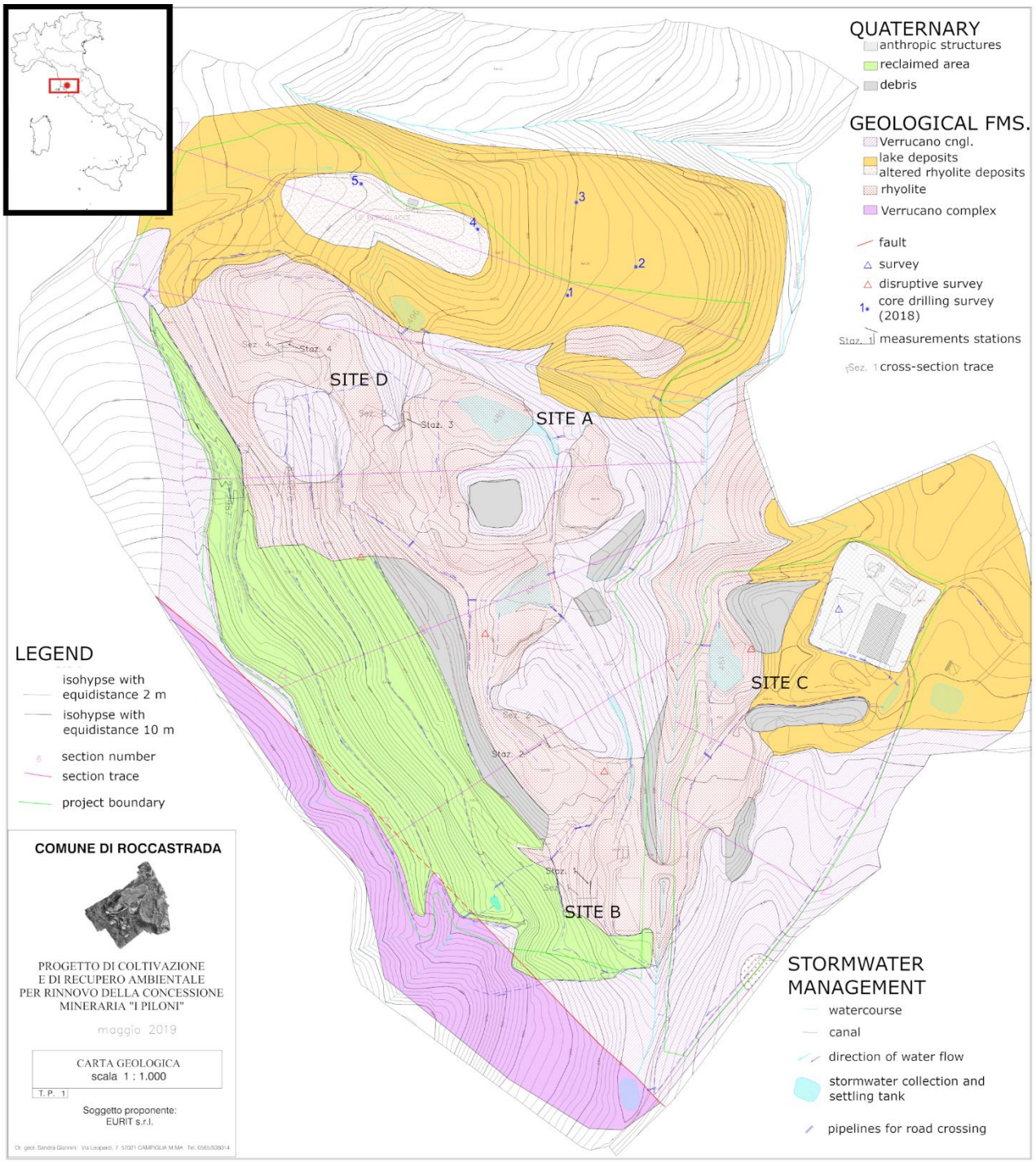

Fig. 1. Geological map of Torniella (I Piloni) mine. Courtesy of EURIT Srl company.

Fig. 2. Kaolin veins, sector B, Torniella (I Piloni) mine.

MATERIALS & METHODS

Kaolin sampled from sector B veins at Torniella (about 2 kg in total) was collected along a fracture front approximately 12 metres long and 10 metres high (scale assessed on the outcrop). The bulk colour of the sample is white, with occasional reddish streaks. Upon handling, it appeared consisting of a bulky, compact component, and a more loose, friable component. The two components were hand separated into two subsamples, KAO_013, the friable part, and KAO_013_BIS, the more compact part (Fig. 3). Both samples were dried in a temperature-controlled oven at 105 °C for 24h to remove moisture and were then ground to fine powders (~0.070 mm) for subsequent analyses.

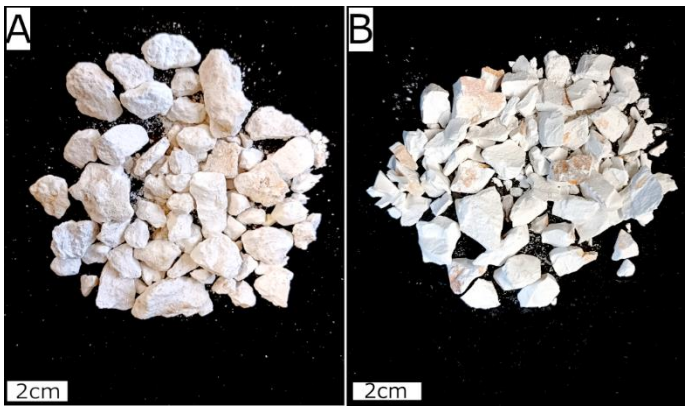

Fig. 3. Kaolin sample from sector B, Torniella (I Piloni) mine: (a) KAO_013 (friable fraction), (b) KAO_013_BIS (compact fraction).

Microtextural, chemical and mineralogical characterization of kaolin

The microtextural and microchemical features of kaolin veins were studied using a Zeiss EVO MA15 scanning electron microscope coupled with an Oxford Aztec 5.0 EDS-EBSD spectrometer (Oxford ULTIM MAX 40 mm^2 EDS and Oxford Symmetry

EBSD) and Oxford INCA250 software. Working conditions were set as follows: accelerating voltage 15 kV, beam current 10 nA, working distance 8.5 mm.

The bulk mineralogical composition of the two samples was assessed by X-ray powder diffraction (XRPD). The analysis was conducted using a XRDynamic 500 diffractometer (Anton Paar), with Cu-Kα radiation (λ = 1.5406 Å, 40 kV, 40 mA) over the 3-90°/2θ range, step size 0.02°/2θ, time per step 60 s. Phase identification was performed using DIFFRAC.EVA (Bruker) software, with the Crystallography Open Database. Semi-quantitative analysis was carried out using DIFFRAC.TOPAS software (Coelho, 2018). Anisotropic broadening is significant in kaolinite (Bish et al., 1989) and was modelled by applying spherical harmonics as implemented in Topas 6 (Dinnebier et al., 2018). Furthermore, XRPD data were also employed to evaluate the structural order-disorder of kaolinite. This parameter is relevant for this study because a higher crystallinity corresponds to a well-ordered lattice with fewer structural defects and stronger cation bonding, which makes cationic exchange increasingly challenging (Pineau et al., 2022). Finally, the mineral phase transformations of the bulk samples upon heating were studied using Thermo-X-Ray Diffraction analysis with a XRDynamic 500 diffractometer (Anton Paar) and a Cu-Kα radiation, ranging 3-70°/2θ, step size of 0.02°, time per step 60 s. The diffractometer was equipped with an Anton Paar HTK-1200N furnace for in situ heating; measurements were performed in air with a heating rate of 10 °C/min.

The bulk chemical characterisation of the samples was performed using X-ray fluorescence spectrometry (XRF). Glass beads with a diameter of 30 mm were prepared in an electric beader from 1 g of sample mixed with 10 g of $Li_2B_4O_7$ flux. The analysis was performed using a ZSX Primus II WD-XRF (Rigaku Industrial Corporation), with a Rh source (4kW, 60mA) in a vacuum chamber. Quantitative analysis of major, minor and trace elements (except Li) was performed using calibration curves created and validated through a large set of international geostandards. Loss on ignition (LOI) was determined by heating three replicates of 0.5 g of each sample at 950 °C for 1.5 hours.

Li contents in the kaolin samples were determined using Inductively Coupled Plasma–Optical Emission Spectrometry (ICP-OES) following a total digestion protocol. This procedure is designed to ensure a gradual and complete dissolution of all mineral phases within the sample matrix. Four representative aliquots (~0.1 g each) of each sample were digested in Teflon vessels on a temperature-controlled hotplate, following sequential heating and evaporation steps using a mixture of concentrated acids (HNO_3, HF, HCl) until complete dissolution was achieved (Balaram & Subramanyyam, 2022). For testing analytical accuracy, digestion was also performed on an international standard reference material (JR1, Geological Survey of Japan). Procedural blank samples were also run to evaluate possible contamination. The final solutions were diluted with MilliQ for elemental analysis on a Thermo Fisher iCAP PRO XP ICP-OES instrument (Thermo Fisher Scientific Inc, Massachusetts, USA), operating with RF power 1.15 kW, nebuliser pressure 5 bar, sample uptake rate 45 rpm, and exposure time 5 s. Measurements were obtained in radial mode using the Li emission line at 670.78 nm. Measurement precision across sample replicates showed a relative standard deviation consistently below 5%, with accuracy to the standard within ±7%.

Leaching tests for Li extraction

Conventional lithium recovery from clays relies on high-temperature mobilisation of Li via exchange with H^+ ions from strong acids (e.g., Zhao et al., 2023), entailing significant environmental and energy impacts. The present study involved the application of procedures aimed at reducing the environmental impact, using reagents with a low ecological footprint to minimise waste toxicity. Specifically, a preliminary compliance test, a room temperature cation exchange test and two calcination and leaching protocols were applied. A further room temperature exchange test using a strong acid was included in order to provide a direct comparison with less sustainable conditions. It is important to note that these tests are of exploratory nature and not intended to be exhaustive.

The preliminary compliance test was conducted in accordance with the European Standard UNI EN 12457-2 (UNI, 2002) for the water leaching of granular waste materials and sludge, using distilled water as the leaching agent with a solid-to-liquid ratio of 5.0 g / 50 mL, and stirring at 300 rpm for 24 h at 21 °C. The room temperature exchange test was carried out using a 1 M $MgCl_2$ solution as the exchange agent, with a solid-to-liquid ratio of 5.0 g / 50 mL, and stirring at 300 rpm for 24 h at 21 °C. The calcination and leaching protocol developed by Zhong et al. (2024) proposes the utilisation of sodium sulfate as an alternative to conventional strong acids, such as H_2SO_4. Sodium sulfate is expected to have a reduced environmental impact and the capacity to promote Li extraction whilst constraining the dissolution of aluminium and iron ions. The procedure was originally applied to a material from the Yuxi mine in Yunnan province (China), containing 0.18 wt% Li_2O, which is said to be mainly present in the kaolinite crystalline structure. A mixture of kaolin (45%) and Na_2SO_4 (55%) was calcined at 800 °C for 90 min with a heating rate of 10 °C/min. The calcined product was then leached in water at a solid-to-liquid ratio of 3.0 g / 15 mL. Leaching was performed at 90 °C for 60 min, with a stirring speed of 300 rpm. The leaching efficiency has been reported to be 84%. The second calcination and leaching test was based on the procedure suggested by Liu et al. (2024), where strong inorganic acids are replaced by a less impacting organic acid such as oxalic acid. The authors treated a complex material composed of chlorite, kaolinite, diaspore, boehmite and muscovite, containing 0.75 wt% Li_2O, where the structural position of lithium remains uncertain. The material was calcined without additives at 600 °C for 60 min (heating rate 10 °C/min) and subsequently leached using a 1.2 M oxalic acid solution at a solid-to-liquid ratio of 1:8. The leaching process was conducted at 80 °C for 180 min, with a stirring speed of 300 rpm. The leaching efficiency reported by Liu et al. was 91%. Finally, an exchange test with a strong acid was conducted at room temperature, employing a 1 M HCl solution as the exchange agent, with a solid-to-liquid ratio of 5.0 g / 50 mL, stirring at 300 rpm for 24 h at 21 °C.

Following centrifugation, Li concentration in each eluate was determined using ICP-OES under the same conditions as those applied for the total lithium content. The recovery of Li was calculated using Equation 1,

$$\varepsilon(Li,\%) = ((c_{Li\ leached} * v_{leached})/(c_{Li\ raw} * m_{bulk\ raw})) * 100 \quad (1)$$

Where ε represents the lithium recovery, *c Li leached* represents the Li concentration in the eluate, *v leached* represents the volume of the eluate, *c Li raw* represents the lithium content in the raw material, *m bulk raw* represents the mass of the sample used in the leaching procedure.

RESULTS

Microtextural, chemical and mineralogical characterization of kaolin

SEM imaging of thin sections of the kaolin veins revealed a microcrystalline texture (Fig. 4a). Semiquantitative EDS analyses indicated the presence of Sr–Al sulfate minerals consistent with svanbergite ($SrAl_3(PO_4)(SO_4)(OH)_6$), occurring both as microcrystalline aggregates and dispersed within the kaolinitic matrix (Fig. 4c, Tab. 1). Locally, As-rich compositions compatible with kemmlitzite ($SrAl_3(AsO_4)(SO_4)(OH)_6$) were also detected.

Bulk XRD analysis of the kaolin-Li-rich samples indicates a composition dominated by kaolinite, with minor quartz and sodic plagioclase in the friable fraction (KAO_013) (Fig. 5). Traces of svanbergite, $SrAl_3(PO_4)(SO_4)(OH)_6$, a mineral of the alunite supergroup, were detected in both samples (Tab. 2). No Li-bearing mineral phases were identified. The determination of the kaolinite crystallinity index (KCI) from X-ray diffraction data is complicated by overlapping peaks from associated minerals and amorphous phases. For example, the widely used Hinckley index (HI) is strongly affected by the presence of quartz, feldspar, iron hydroxide gels, illite, smectite and halloysite (Aparicio & Galan, 1999). Consequently, the KCI could not be calculated for KAO_013 due to the presence of interfering accessory phases, namely quartz. For KAO_013_BIS, the Aparicio-Galán-Ferrell index (AGFI) was determined by fitting the peak heights of the 020, 1-10 and 11-1 reflections of kaolinite. The calculated AGFI is 0.7, indicative of a highly defective kaolinite (Aparicio et al., 2006). For comparison, the Hinckley Index (HI), based on the intensity of the same reflections, returned a value of 0.8, corresponding to a medium-defect kaolinite structure (Hinckley, 1962) (Tab. 2). Thermo-XRD analyses of the two kaolin samples show, as expected, that the characteristic 001 peak of kaolinite (7.2 Å) starts decreasing its intensity above 500 °C due to dehydroxylation, and is completely missing at 600 °C, possibly indicating the formation of metakaolinite (X-ray amorphous phase) (Fig. 6). At the same temperature, svanbergite is no longer detected, as it underwent dehydration and loss of crystallinity.

XRF analyses of the two kaolin samples showed similar chemical compositions in terms of major and minor oxides, as well as trace elements (Tab. 3, Tab. 4). The dominance of silica and alumina is fully consistent with a mineralogical composition dominated by kaolinite. The relatively elevated Sr concentrations measured in both samples are attributable to the presence of Sr-Al sulfates, as identified by XRPD.

The total Li content of the kaolin samples considered for the present explorative study was measured with ICP-OES and resulted in 1667 mg/kg for KAO_013 and 3556 mg/kg for KAO_013_BIS (Tab. 4).

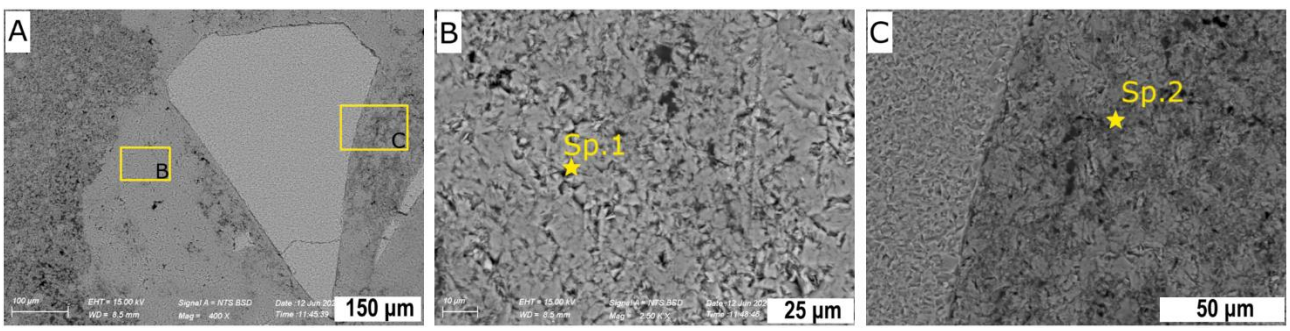

Fig. 4. SEM secondary electron (SE) images of kaolin vein sample. Sp. 1 and Sp. 2 correspond to the points where EDS microanalyses were conducted. The semiquantitative composition (see Tab. 1) suggests for Sp.1 a Si-Al composition compatible with kaolinite; whereas Sp.2 suggests the presence of svanbergite (darker spots in Fig. 6c) in the kaolinitic matrix.

CHEMICAL COMPOSITION [wt%]	Al_2O_3	SiO_2	P_2O_5	SO_4	K_2O	SrO
KAO_003_Sp.1	46.7	53.3	-	-	-	-
KAO_003_Sp.2	37.6	15.6	11.4	16.0	0.6	15.3

Tab. 1. Semiquantitative composition of kaolin vein sample obtained with SEM-EDS measurements.

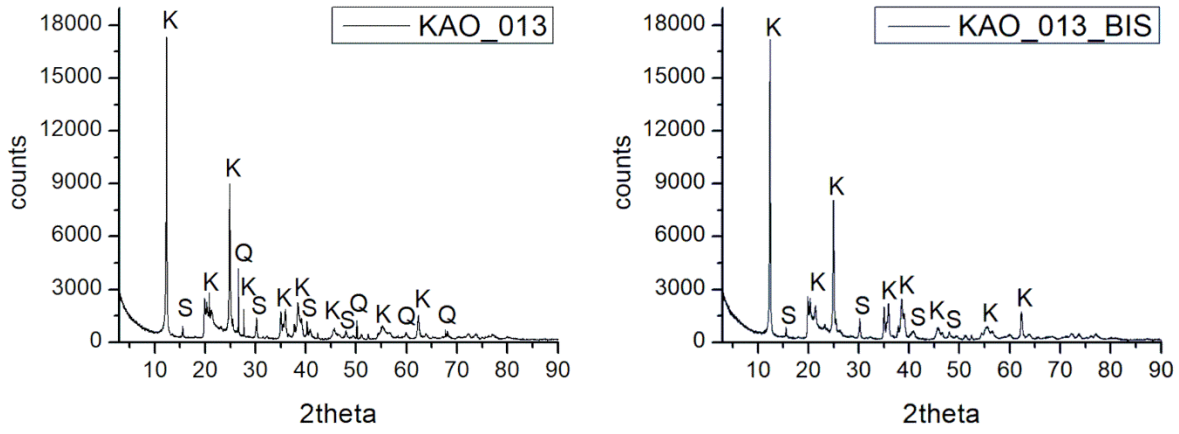

Fig. 5. XRD patterns for KAO_013 and KAO_013_BIS bulk raw powders; peak identification: K = kaolinite, S = svanbergite, Q = quartz.

XRPD bulk semiquantitative analysis					kaolinite crystallinity index	
	clays (kaolinite)	alunite supergroup minerals	quartz	plagioclase	AGFI	HI
KAO_013	89%	3%	7%	<2%	N/A	N/A
KAO_013_BIS	97%	3%	<DL	<DL	0.7	0.8

Tab. 2. Bulk mineralogical composition of the kaolin samples (error 3-5%; LOD ~1%). Kaolinite crystallinity calculated with AGFI and HI indices.

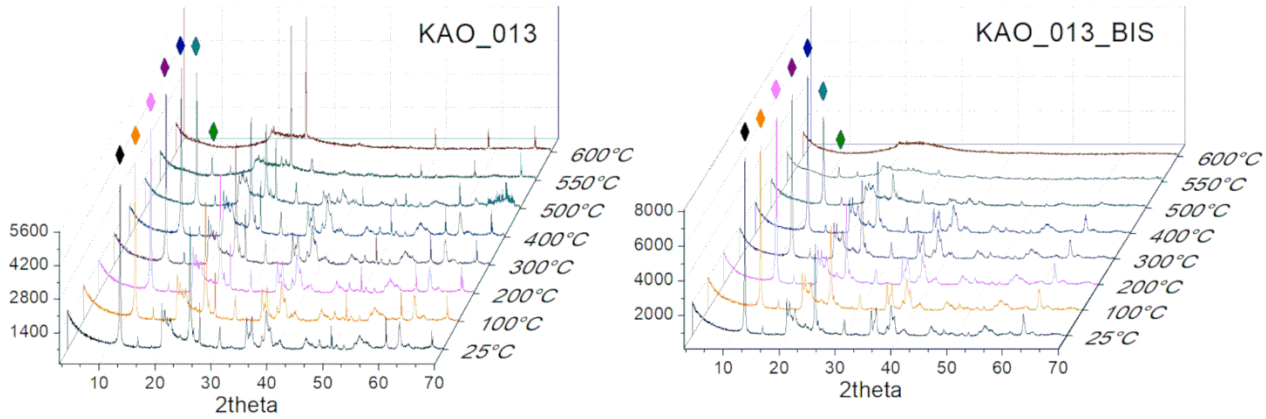

Fig.6. Thermo-XRD analysis results for KAO_013 and KAO_013_BIS, in the range of 25-600 °C. The kaolinite 001 peak is indicated for each diffractogram, if present.

ANALYTE	SiO_2	Al_2O_3	Fe_2O_3	MnO	MgO	CaO	Na_2O	K_2O	TiO_2	P_2O_5	SrO	LOI	TOT	SO_3 *
UNIT	wt%	wt%	wt%	wt%	wt%	wt%	wt%	wt%	wt%	wt%	wt%	%	-	wt%
DL	0.50	0.80	0.03	$2*10^{-3}$	0.03	0.02	0.30	0.02	0.01	0.02	$0.5*10^{-3}$	-	-	-
KAO_013	43.88	38.46	0.39	0.01	<DL	0.07	<DL	0.14	0.11	0.53	0.97	14.66	99.21	0.75
KAO_013_BIS	40.14	41.65	0.17	0.01	<DL	0.07	<DL	0.08	0.03	0.57	1.06	15.10	98.87	0.82

Tab. 3. Major and minor oxide composition of the bulk kaolin samples. DL indicates the detection limit. * SO3 contents correspond to the amount estimated to be present in svanbergite, calculated from the measured Sr concentrations; this contribution is included in the reported LOI values.

ANALYTE	V	Cr	Ni	Cu	Zn	Zr	Ba	Co	Rb	Y	Nb	Li *
UNIT	mg/kg	mg/kg	mg/kg	mg/kg	mg/kg	mg/kg	mg/kg	mg/kg	mg/kg	mg/kg	mg/kg	mg/kg
LOD	3	10	5	3	3	5	30	5	5	20	30	$0.5*10^{-3}$
KAO_013	52	69	59	78	4	27	272	5	14	<DL	<DL	1712 ± 49
KAO_013_BIS	69	63	59	50	4	<DL	327	6	<DL	<DL	<DL	3628 ± 90

Tab. 4. Trace element contents in the bulk kaolin samples. DL indicates the detection limit. * Li content analysed by ICP-OES (emission line 670.78 nm), reported as the mean value between four different aliquots of the sample.

Leaching tests for Li extraction

The compliance test, the cation exchange test, and the room temperature leach with a 1M HCl yielded very low Li release. Specifically, the compliance test conducted in accordance with the European Standard UNI EN 12457-2 (room temperature batch reaction with pure water) showed a Li release of only 0.1% for both samples. The room temperature exchange test in a 1M $MgCl_2$ solution achieved a recovery of Li of 0.2% for KAO_013 and KAO_013_BIS (Tab. 5). Finally, the room temperature exchange test in a 1M HCl solution achieved a recovery of Li of 0.4% for both samples (Tab. 5). Calcination of the kaolin samples at 800 °C with Na_2SO_4 and water leaching at 90 °C, yielded Li recoveries of 37% for KAO_013 and 22% for KAO_013_BIS (Tab. 5). XRPD analyses of the calcined powders revealed residual quartz and sodium sulfate phases in KAO_013, whereas only the sodium sulfate pattern was detected in KAO_013_BIS. This indicates that both kaolinite and svanbergite underwent complete transformation during the calcination process. However, Li extraction efficiencies remained comparatively low in relation to the findings reported by Zhong et al. (2024). In contrast, calcination at 600 °C without additives, followed by leaching in oxalic acid solution at 80 °C, resulted in significantly higher Li recovery rates, although these were still below the values reported by Liu et al. (2024): 58% for KAO_013 and 53% for KAO_013_BIS (Tab. 5). XRPD analyses of the calcined powders revealed residual quartz in KAO_013, whereas KAO_013_BIS was found to be completely amorphous.

	Room temperature exchange in $MgCl_2$ solution	Calcination with Na_2SO_4 + hot leaching in water solution	Calcination + hot leaching in oxalic acid solution	Room temperature exchange in HCl solution
KAO_013	0.2%	37%	58%	0.4%
KAO_013_BIS	0.2%	22%	53%	0.4%

Tab. 5. Li recovery (%) after exchange tests and leaching processes.

DISCUSSION

Kaolinite-rich veins from the Torniella rhyolite mine locally contain remarkably high Li contents, ranging from 1600 to 3700 mg/kg, with local enrichment of up to 6000 mg/kg. These concentrations are significantly higher than those observed in the hosting rocks. Previous studies (summarised in Lattanzi et al., 2001) suggest a structurally controlled hydrothermal alteration by ascending fluids, possibly originated in a steam-heated environment. There is no specific evidence about the Li-hosting phase(s) in the unaltered rhyolite. The most probable candidates involved in Li mobilisation during hydrothermal alteration are biotite and the glass phase (e.g. Ellis et al., 2022). Thus, vein minerals, and specifically kaolinite, may have concentrated the Li mobilised from rhyolite alteration. Kaolinite has been identified as the most probable host phase for lithium within the veins, although direct evidence of Li structural position is currently lacking. Li contents in Torniella kaolin veins are among the most relevant documented for this mineral, and of the same order of magnitude of grades considered economic in some clay-type Li deposits (Bowell et al., 2020; Xie et al., 2024). Exchange tests at room temperature in pure water, $MgCl_2$ 1M and HCl 1M resulted in low extraction efficiencies, approximately 0.2 - 0.4%. These results suggest that Li is not simply adsorbed onto the kaolinite structure (e.g., surface defects), otherwise it would have reacted to the mild exchange conditions, being released in the solution upon substitution with H^+ or Mg^{2+}. The thermally induced transformations of kaolinite during calcination appear to play a key role in enhancing Li extraction efficiency. Between 400 °C and 600 °C, kaolinite undergoes dehydroxylation and structural collapse of its layered sheets, leading to the formation of metakaolin. This behaviour was confirmed by thermo-XRD analyses, which indicate that the transformation from kaolinite to X-ray amorphous phases in the Torniella samples is complete at 600 °C. High-temperature transformations have been shown to enhance reactivity and Li mobility (Dhar & Bishnoi, 2024; Liu et al., 2024). Indeed, leaching tests following calcination yielded significant Li extraction, although considerably lower than the >80% efficiencies documented in the reviewed literature. Despite the lower calcination temperature of 600 °C, the combination of heating without additives followed by hot leaching in oxalic acid solution resulted in a higher Li recovery than the calcination at 800 °C with Na_2SO_4, followed by hot water leaching. These results suggest that the exchange between H^+ from the oxalic acid and Li^+ is favoured in comparison to the exchange of lithium with Na^+ from sodium sulfate. The experimental procedures were conducted under conditions described as optimal in the extant literature, including reagent concentrations, calcination temperature and duration, as well as leaching time and temperature (Liu et al., 2024; Zhong et al., 2024). The present study did not investigate whether alternative conditions, such as higher calcination temperatures or extended reaction times, may yield enhanced Li extraction efficiencies for Torniella kaolin samples. Furthermore, although kaolin represents the primary material in both the consulted literature and the present study, variations in accessory mineral phases may influence the overall extraction behaviour. At this stage, given the exploratory nature of the study, the pursuit of parameter optimisation was not deemed to be a priority. These results, although preliminary, suggest that Li-rich kaolinite may represent a potential unconventional source of Li, particularly in the context of by-product recovery from kaolin extraction.

CONCLUSIONS

The rhyolite bodies currently exploited at the Torniella (*I Piloni*) mine, one of the most significant ceramic raw material deposits in Italy, exhibit a moderate Li anomaly (up to 160 mg/kg), a characteristic that is commonly observed in the Tertiary Tuscan magmatic province. Conversely, a sector of the mine is distinguished by the occurrence of centimetric veins, predominantly composed of kaolinite, which exhibit significantly higher Li contents (1600 - 3700 mg/kg, with local enrichment up to 6000 mg/kg). Preliminary tests of Li recovery demonstrated a limited mobility of the metal. Room temperature reaction with water, $MgCl_2$ and HCl, released approximately 0.2 - 0.4% Li, indicating that the metal is not weakly adsorbed, but structurally bound. Thermal treatment and hot leaching yielded better results (22 - 58%), even if lower than those reported in the literature for the same procedures. Specifically, the most positive results (up to ∼60% recovery) were obtained with calcination at 600 °C and hot leaching with oxalic acid. This technique has been shown to outperform calcination with Na_2SO_4 at 800 °C and water leaching, suggesting that H^+ exchange in acidic conditions is more effective than Na^+-based mechanisms. Additional optimisation of process parameters, including temperature, duration, and reagent concentration, may yield better outcomes. At the current state of knowledge, the lithium resource appears negligible, being limited to a small portion of the Torniella mine. Furthermore, the presence of sulfur compounds (svanbergite, kemmlitzite) penalises the kaolin residue for ceramic applications. Although not currently economically viable, the results of this study demonstrate a concrete potential for Li recovery as a by-product from Li-rich kaolin. The final goal is to develop processes that preserve the properties of kaolin for post-leaching industrial applications, paving the way for integrated resource recovery strategies. Future works would focus on optimising extraction conditions and investigating the structural position of lithium within the kaolinitic matrix by means of advanced analytical techniques.

ACKNOWLEDGEMENTS

S.R. acknowledges that recent investigations on alternative lithium sources have been made possible through the support of the projects: “Sviluppo di un processo di sepARazione innovativo per la valorizzazione degli inerti contenenti materiali sTrategici per l'industria eUropea – ARTÙ” funded by Regione Toscana within the framework of the FESR 2021–2027 Program - Progetti Strategici di Ricerca e Sviluppo and “LiCycle” funded by the University of Florence under the Progetti Competitivi Biennali per Ricercatori a Tempo Determinato (RTD) program for 2025–2026. The authors acknowledge Iris Belfiore (University of Florence) for her kind support during the laboratory leaching experiments.

REFERENCES

Aparicio, P., Galán, E. (1999) - Mineralogical Interference on Kaolinite Crystallinity Index Measurements. Clays Clay Miner. 47, 12–27. https://doi.org/10.1346/CCMN.1999.0470102.

312 Aparicio, P., Galán, E. & Ferrell, R. E. (2006) - A new kaolinite order index based on XRD profile fitting. Clay Miner., 41(4), 811-817.
313 https://doi.org/10.1180/0009855064140220.
314 Balaram, V. & Subramanyam, K. S. V. (2022) - Sample preparation for geochemical analysis: Strategies and significance. Adv. Sample
315 Prep., 1, 100010. https://doi.org/10.1016/j.sampre.2022.100010.
316 Benson, T. R., Coble, M. A. & Dilles, J. H. (2023) - Hydrothermal enrichment of lithium in intracaldera illite-bearing claystones. Sci.
317 Adv., 9(35), eadh8183. https://doi.org/10.1126/sciadv.adh8183.
318 Benson, T. R., Jowitt, S. M. & Simon, A. C. (2025) - Special issues on the geology and origin of lithium deposits—introduction: Lithium
319 deposit types, sizes, and global distribution. Econ. Geol., 120(3), 503-511. https://doi.org/10.5382/econgeo.5149.
320 Bertolani M. & Loschi Ghittoni A.G. (1989) - Kaolin of Piloni di Torniella (Tuscany). Ind. Mineraria, 40, 19-27.
321 Bish, D. L. & Von Dreele, R. B. (1989) - Rietveld refinement of non-hydrogen atomic positions in kaolinite. Clays Clay Miner., 37(4),
322 289-296. https://doi.org/10.1346/CCMN.1989.0370401.
323 Bodart, P., Delmotte, L. , Rigolet, S., Brendle, J. & Gougeon, R. (2018) - 7 Li { 19 F} TEDOR NMR to observe the lithium migration in
324 heated montmorillonite. Appl. Clay Sci., 157, 204 - 211. https://dx.doi.org/10.1016/j.clay.2018.03.007.
325 Bowell, R. J., Lagos, L., de los Hoyos, C. R. & Declercq, J. (2020) - Classification and characteristics of natural lithium resources.
326 Elements, 16(4), 259-264. https://doi.org/10.2138/gselements.16.4.259.
327 Coelho, A. A. (2018) - TOPAS and TOPAS-Academic: an optimization program integrating computer algebra and crystallographic
328 objects written in C++. J. Appl. Crystallogr., 51(1), 210-218. https://doi.org/10.1107/S1600576718000183.
329 Cortecci, G., Lombardi, G., Reyes, E. & Turi, B. (1981) - A sulfur isotopic study of alunites from Latium and Tuscany, Central Italy.
330 Miner. Depos., 16, 147-156. https://doi.org/10.1007/BF00206460.
331 Dhar, M. & Bishnoi, S. (2024) - Influence of calcination temperature on the physical and chemical characteristics of kaolinitic clays
332 for use as supplementary cementitious materials. Cem. Concr. Res., 178, 107464.
333 https://doi.org/10.1016/j.cemconres.2024.107464.
334 Dini, A., Lattanzi, P., Ruggieri, G. & Trumpy, E. (2022) - Lithium Occurrence in Italy - An Overview. Miner., 12(8), 945.
335 https://doi.org/10.3390/min12080945.
336 Dinnebier, R. E., Leineweber, A. & Evans, J. S. (2018) - Rietveld refinement: practical powder diffraction pattern analysis using TOPAS.
337 Walter de Gruyter GmbH & Co KG. https://doi.org/10.1515/9783110461381.
338 Ellis, B. S., Szymanowski, D., Harris, C., Tollan, P.M.E., Neukampf, J., Guillong, M., Cortes-Calderon, E.A. & Bachmann, O. (2022) -
339 Evaluating the Potential of Rhyolitic Glass as a Lithium Source for Brine Deposits. Econ. Geol., 11(1), 91–105.
340 https://doi.org/10.5382/econgeo.4866.
341 European Parliament (2024) - Regulation (EU) 2024/1252 of the European Parliament and of the Council of 11 April 2024 establishing
342 a framework for ensuring a secure and sustainable supply of critical raw materials and amending Regulations (EU) No 168/2013,
343 (EU) 2018/858, (EU) 2018/17. Off. J. Eur. Union, 1–67. March. https://eur-lex.europa.eu/eli/reg/2024/1252/oj.
344 Finto, G. (2025) - Caratterizzazione di sfridi di cava e prodotti industriali non conformi per la valutazione del potenziale estrattivo del
345 litio. https://sol.unifi.it/tesi/consultazione.

Hao, H., Jiu, B., Huang, W., Yu, C., Wang, Z., Qin, B. & Huang, L. (2025) - The role of geological fluids on the distribution of lithium in anthracite, an example from the Yangquan Mining District, Qinshui Basin, northern China. Int. J. Coal Geol., 303, 104754. https://doi.org/10.1016/j.coal.2025.104754.

Hedenquist, J. W., Arribas, A. (2022) - Exploration Implications of Multiple Formation Environments of Advanced Argillic Minerals. Econ. Geol., 117(3), 609–643. https://doi.org/10.5382/econgeo.4880.

Hinckley, D. N. (1962) - Variability in "crystallinity" values among the kaolin deposits of the coastal plain of Georgia and South Carolina. Clays Clay Miner., 11, 229-235. https://doi.org/10.1346/CCMN.1962.0110122.

Hindshaw, R. S., Tosca, R., Goût, T. L., Farnan, I., Tosca, N. J. & Tipper, E. T. (2019) - Experimental constraints on Li isotope fractionation during clay formation. Geochim. Cosmochim. Acta, 250, 219-237. https://doi.org/10.1016/j.gca.2019.02.015.

Hoyer, M., Kummer, N. A. & Merkel, B. (2015) - Sorption of Lithium on Bentonite, Kaolin and Zeolite. Geosciences, 5(2), 127-140. https://doi.org/10.3390/geosciences5020127.

Hu, Z. & Gao, S. (2008) - Upper Crustal Abundances of Trace Elements: A Revision and Update. Chem. Geol., 253, 205-221. https://doi.org/10.1016/j.chemgeo.2008.05.010.

Lattanzi, P., Benvenuti, M., Costagliola, P., Maineri, C., Mascaro, I., Tanelli, G., Dini, A. & Ruggieri, G. (2001) - Magmatic versus hydrothermal processes in the formation of raw ceramic material deposits in southern Tuscany. In: Cidu, R. (ed), Water-rock interaction: proceedings of the Tenth International Symposium on water-rock interaction, A. A. Balkema, 725-728.

Liu, J., Xu, R., Sun, W., Wang, L. & Zhang, Y. (2024) - Lithium Extraction from Lithium-Bearing Clay Minerals by Calcination-Leaching Method. Miner., 14(3), 248. https://doi.org/10.3390/min14030248.

Lombardi, G. & Mattias, P.P. (1987) - The kaolin deposits of Italy. Ind. mineraria, Serie III, VIII(6), 1-34.

Mazzuoli, G., (1967) - Le vulcaniti di Roccastrada (Grosseto). Studio chimico petrografico e geologico. Atti Soc. Tosc. Sci. Nat., Mem., Serie A. 74(2), 315-373.

Pinarelli, L., Poli, G. & Santo, A.P. (1989) - Geochemical characterization of recent volcanism from the Tuscan Magmatic Province (Central Italy): the Roccastrada and San Vincenzo centers. Period. Mineral., 58, 67-96.

Pineau, M., Mathian, M., Baron, F., Rondeau, B., Deit, L.L., Allard, T. & Mangold, N. (2021) - Estimating kaolinite crystallinity using near-infrared spectroscopy: Implications for its geology on Earth and Mars. Am. Mineral., 107, 1453-1469. https://doi.org/10.2138/am-2022-8025.

Putzolu, F., Armstrong, R. N., Boyce, A. J., Hepburn, L. E., Bompard, N., Najorka, J., Lefebvre-Desanois M., Milton A. J., Salge T., Erak D., Abad I. & Herrington, R. J. (2025) - Origin of the Jadar volcano-sedimentary Li-B deposit, Serbia. Econ. Geol., 120(3), 599-625. https://doi.org/10.5382/econgeo.5132.

Rye, R. O., Bethke, P. M. & Wasserman, M. D. (1992) - The stable isotope geochemistry of acid-sulfate alteration. Econ. Geol., 87, 225-262. https://pubs.usgs.gov/of/1991/0257/report.pdf.

Sammuri, P. & Scapigliati W. (2022) - La miniera di caolino del Monte Alto a Piloni di Torniella (Roccastrada, Grosseto): geologia e storia industriale dell'area estrattiva. Atti Soc. Tosc. Sci. Nat., Mem., Serie A, 129, 65-80. https://doi.org/10.2424/ASTSN.M.2022.07.

Starkey, H. C. (1982) - The role of clays in fixing lithium. Bull. U.S. Geol. Surv., 1278, iii, F1-F11. https://doi.org/10.3133/b1278F.

U.S. Geological Survey (2026) - Mineral commodity summaries 2026 (ver. 1.1, March 2026). Bull. U.S. Geol. Surv., 222. https://doi.org/10.3133/mcs2026.

UNI - Ente Italiano di Normazione (2002) - EN 12457-2:2002. https://store.uni.com/en-12457-2-2002.

Viti, C., Lupieri, M. & Reginelli, M. (2007) - Weathering sequence of rhyolitic minerals: the kaolin deposit of Torniella (Italy). Neues Jahrb. Mineral. Abh., 183(2), 203-213. https://doi.org/10.1127/0077-7757/2007/0072.

Xie, R., Zhao, Z., Tong, X., Xie, X., Song, Q. & Fan, P. (2024) - Review of the research on the development and utilization of clay-type lithium resources. Particuology, 87, 46-53. https://doi.org/10.1016/j.partic.2023.07.009.

Yan, S., Cui, Y., Cheng, Y., Cai, Y., Li, W., Hong, J., Zhao, Y., Li, J., Yang, X., Sun, T., Yu, J., Zhang, X., Zhang, H., Yuan, Y., Xu, J., Huang, S. & Gan, R. (2025) - Occurrence State of Lithium in Clay Minerals Based on Element-Complexation Mechanisms. Langmuir, 41(43), 28934−28947. https://doi.org/10.1021/acs.langmuir.5c01735.

Yan, S., Li, W., Cai, Y., Yuan, Y., Zou, Q., Wang, J., Zhang, X., Fang, Z., Zhang, H., Sun, T., Li, W. & Yu, J. (2026) - Molecular-level insights into mechanisms of Li enrichment and occurrence in natural clay-bauxite. Am. Mineral., 111(3), 446-460. https://doi.org/10.2138/am-2024-9683.

Zhao, H., Wang, Y. & Cheng, H. (2023) - Recent advances in lithium extraction from lithium-bearing clay minerals. Hydrometallurgy, 217, 106025. https://doi.org/10.1016/j.hydromet.2023.106025.

Zhong, W., Feng, H., Tong, L., Li, D., Yang, L. & Rao, F. (2024) - Lithium extraction from a Li-rich kaolin resource through Na2SO4 roasting and water leaching. Miner. Eng., 218, 109004. https://doi.org/10.1016/j.mineng.2024.109004.